J. Plasma Fusion Res. SERIES, Vol. 6 (2004) 152–155

Analysis of the MHD Instability Driving Mechanism in 3D Heliotron and Quasiaxisymmetric Systems

COOPER W. Anthony, NARUSHIMA Yoshiro[1], WATANABE Kiyomasa[1], YAMAZAKI Kozo[1], SUZUKI Chihiro[1] and OKAMURA Shoichi[1]

Centre de Recherches en Physique des Plasmas, EPFL, Lausanne, Switzerland

[1]National Institute for Fusion Science, Toki 509-5292, Japan

(Received: 9 December 2003 / Accepted: 22 March 2004)

Abstract

A module for the three dimensional (3D) ideal magnetohydrodynamic (MHD) code TERPSICHORE has been formulated and implemented to investigate the driving and stabilising mechanisms associated with global and local ideal MHD modes in 3D magnetic confinement systems. The energy principle that describes the MHD stability behaviour is expressed as $\delta W_P = (1/2) \iiint d^3x\, (C^2 - D|\xi^s|^2)$, where C^2 is the stabilising element due to the compression and bending of magnetic field lines, whereas the instability driving term is $D|\xi^s|^2$ which can be separated into two components. One of these components is proportional to the pressure gradient responsible for local ballooning and Mercier modes. The second component is proportional to the parallel current density $\boldsymbol{j}\cdot\boldsymbol{B}/B^2$. This term is responsible for global internal and external kink modes. However, in finite β plasmas, the surface varying component of $\boldsymbol{j}\cdot\boldsymbol{B}/B^2$ is proportional to the pressure gradient. Although this could complicate the distinction between ballooning and surface varying parallel current driven kinks, it is found that the perturbed energy structures each generate are different in character. In addition, the average and surface varying contributions of $\boldsymbol{j}\cdot\boldsymbol{B}/B^2$ to δW_P can be evaluated separately. Applications to a currentless 10-period Heliotron demonstrates that the ballooning-interchange mechanism is dominant in destabilising ideal MHD modes. In a 2-period quasiaxisymmetric device with finite bootstrap current, the kink mode mechanism driven by the surface varying component of $\boldsymbol{j}\cdot\boldsymbol{B}/B^2$ is dominant near marginal stability.

Keywords:

ideal MHD energy principle, stellarators, quasi-axisymmetry (QAS), instability drive, Pfirsch-Schlüter current, 3D equilibrium and stability code

1. Introduction

Ideal magnetohydrodynamic (MHD) instabilities impose limits on the β value that can be achieved in magnetically confined plasmas. The bending and compression of field lines balance the interaction of the pressure gradient with the magnetic field line curvature that drives ballooning-interchange modes and the parallel current density that drives internal and external kink modes. A diagnostic code is developed to analyse the driving and stabilising terms of the internal plasma potential energy δW_P. The driving terms can be separated into pressure gradient ballooning-interchange δW_D and parallel current density δW_J contributions. The Pfirsch-Schlüter current is related to the flux surface varying component of the parallel current density and is proportional to the pressure gradient. A finite flux surface average component of the parallel current density is a consequence of bootstrap (BC), ohmic (OH) or electron cyclotron current drive (ECCD) currents. A rough identification of Pfirsch-Schlüter driven kinks and kink modes driven by BC, OH or ECCD is undertaken by suppressing the contribution of one or the other in δW_J. Applications to a 10-period currentless Heliotron [1] and a 2-period quasiaxisymmetric (QAS) [2] stellarator reactor with finite bootstrap-like current are investigated.

2. The components of the energy principle

The incompressible ideal MHD stability problem is reduced to the solution of the equation $\delta W_P + \delta W_V - \omega^2 \delta W_K = 0$, where δW_P is the internal plasma potential energy, δW_V is the energy in the vacuum region surrounding the plasma, $-\omega^2 \delta W_K$ is the kinetic energy and ω^2 is the eigenvalue. In Boozer magnetic coordinates [3], expressions for δW_P, δW_V and δW_K described in Ref. [4] have been implemented in the 3D TERPSICHORE stability code [5]. The driving terms of δW_P can be separated into a pressure gradient p' component

Corresponding author's e-mail: wilfred.cooper@epfl.ch

$$\delta W_D = -\frac{1}{2}\int_0^1 ds \int_0^{\frac{2\pi}{L_s}} d\phi \int_0^{2\pi} d\theta \, p'(s)$$
$$\times \left[\frac{\sqrt{g}\,p'(s)}{B^2} - \frac{\partial\sqrt{g}}{\partial s} + \frac{J(s)\psi''(s) - I(s)\Phi''(s)}{B^2} \right] (\xi^s)^2$$
$$+\frac{1}{2}\int_0^1 ds \int_0^{\frac{2\pi}{L_s}} d\phi \int_0^{2\pi} d\theta \, p'(s) \frac{B_s}{B^2}\sqrt{g}\; B\cdot\nabla(\xi^s)^2$$

and a parallel current density $\boldsymbol{j}\cdot\boldsymbol{B}/B^2$ component

$$\delta W_J = -\frac{1}{2}\int_0^1 ds \int_0^{\frac{2\pi}{L_s}} d\phi \int_0^{2\pi} d\theta \frac{\boldsymbol{j}\cdot\boldsymbol{B}}{B^2}$$
$$\times \left[\frac{\sqrt{g}B^2}{|\nabla s|^2}\left(\frac{\boldsymbol{j}\cdot\boldsymbol{B}}{B^2}\right) + \psi'(s)\Phi''(s) - \Phi'(s)\psi''(s) \right] (\xi^s)^2$$
$$+\frac{1}{2}\int_0^1 ds \int_0^{\frac{2\pi}{L_s}} d\phi \int_0^{2\pi} d\theta \frac{j\cdot B}{B^2}$$
$$\times \left[\frac{I(s)}{|\nabla s|^2}\frac{g_{s\theta}}{\sqrt{g}} + \frac{J(s)}{|\nabla s|^2}\frac{g_{s\phi}}{\sqrt{g}} \right] \sqrt{g} B\cdot\nabla(\xi^s)^2$$

The stabilising contribution then is extracted by evaluating $\delta W_{C^2} = \delta W_P - \delta W_D - \delta W_J$ and must be verified to be positive-definite everywhere. The flux surface averaged component of $\boldsymbol{j}\cdot\boldsymbol{B}/B^2$ is given, as calculated in a Boozer magnetic coordinate reference frame by the expression $[J(s)I'(s) - I(s)J'(s)]/[\psi'(s)J(s) - \Phi'(s)I(s)] = (\boldsymbol{j}\cdot\boldsymbol{B}/B^2)_{00}$, where $J(s)$ and $I(s)$ are the toroidal and poloidal current flux functions, respectively and $\Phi(s)$ and $\psi(s)$ are the toroidal and poloidal magnetic flux functions, respectively. Primes ($'$) indicate derivatives with respect to the radial variable s. By suppressing the flux surface varying component of $\boldsymbol{j}\cdot\boldsymbol{B}/B^2$ associated with the Pfirsch-Schlüter current, we can estimate the impact of bootstrap, ohmic or ECCD currents to the kink driving term by evaluating

$$\delta W_{J0} = -\frac{1}{2}\int_0^1 ds \int_0^{\frac{2\pi}{L_s}} d\phi \int_0^{2\pi} d\theta \left(\frac{\boldsymbol{j}\cdot\boldsymbol{B}}{B^2}\right)_{00}$$
$$\times \left[\frac{\sqrt{g}B^2}{|\nabla s|^2}\left(\frac{\boldsymbol{j}\cdot\boldsymbol{B}}{B^2}\right)_{00} + \psi'(s)\Phi''(s) - \Phi'(s)\psi''(s) \right] (\xi^s)^2$$
$$+\frac{1}{2}\int_0^1 ds \int_0^{\frac{2\pi}{L_s}} d\phi \int_0^{2\pi} d\theta \left(\frac{j\cdot B}{B^2}\right)_{00}$$
$$\times \left[\frac{I(s)}{|\nabla s|^2}\frac{g_{s\theta}}{\sqrt{g}} + \frac{J(s)}{|\nabla s|^2}\frac{g_{s\phi}}{\sqrt{g}} \right] \sqrt{g} B\cdot\nabla(\xi^s)^2.$$

The difference between δW_J and δW_{J0} yields an estimate of the impact of the Pfirsch-Schlüter current as a driving mechanism for kink modes.

3. Application to currentless 10-period Heliotron

We analyse the different contributions to the Energy Principle in a current-free 10-period Heliotron [6]. The profiles for δW_P, δW_{C^2}, δW_D and δW_J are shown in Fig. 1 for a case with $\beta \simeq 2\%$. The ballooning-interchange driving mechanism δW_D dominates over the parallel current driving mechanism δW_J for the most unstable mode of the system, a $m/n = 3/2$ structure. As anticipated, the stabilising δW_{C^2} term is positive everywhere. We have also verified that the reconstructed δW_P profile reproduces exactly the profile calculated spectrally in the TERPSICHORE code. An analysis of the full 3D distribution of the different components of the Energy Principle is also instructive. We present the

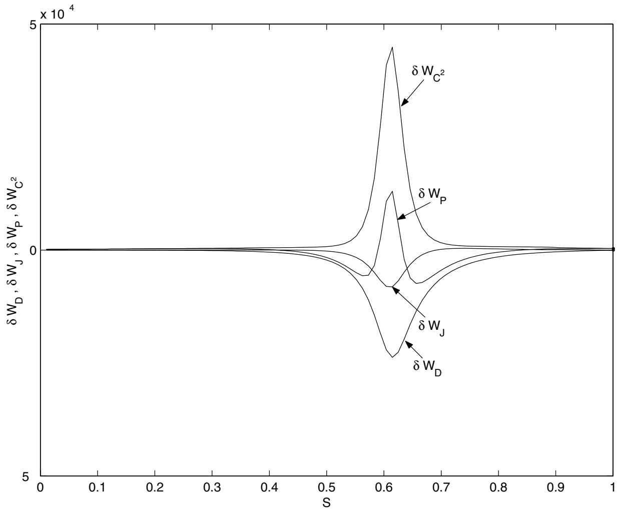

Fig. 1 The stabilising (δW_{C^2}), the internal plasma potential energy (δW_P), the kink (δW_J) and the ballooning-interchange (δW_D) profiles in a currentless 10-period Heliotron. The curves labelled from top to bottom are δW_{C^2}, δW_P, δW_J and δW_D, respectively.

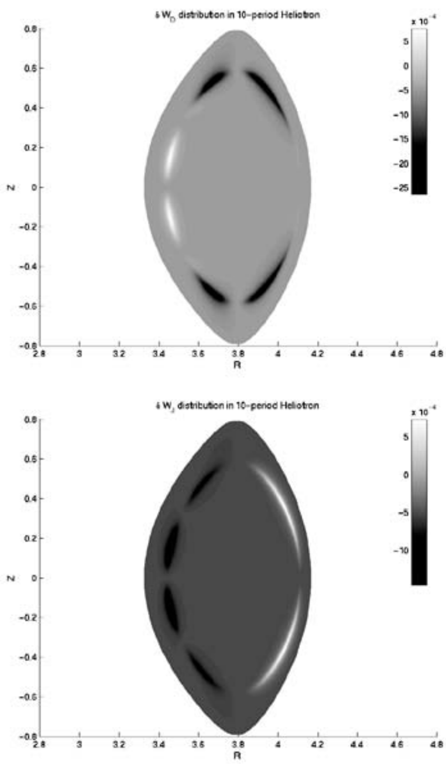

Fig. 2a The structure of the integrands of the functionals δW_D (top) and δW_J (bottom) for a 10-period currentless Heliotron on a toroidal cross section at the beginning of a period ($\phi = 0$). The scale for δW_D is $-2.6 \times 10^{-3} < \delta W_D < 7 \times 10^{-4}$ and the scale for δW_J is $-1.4 \times 10^{-3} < \delta W_J < 7 \times 10^{-4}$.

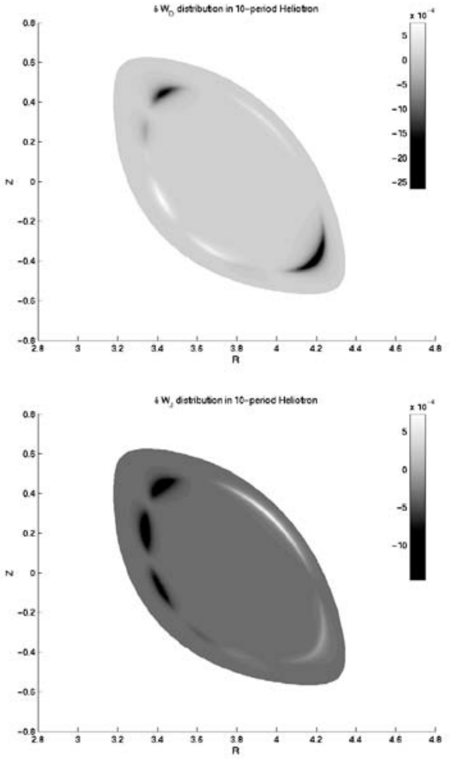

Fig. 2b The structure of the integrands of the functionals δW_D (top) and δW_J (bottom) for a 10-period currentless Heliotron on a toroidal cross section at one quarter of a period ($\phi = \pi/20$). The scale for δW_D is $-2.6 \times 10^{-3} < \delta W_D < 7 \times 10^{-4}$ and the scale for δW_J is $-1.4 \times 10^{-3} < \delta W_J < 7 \times 10^{-4}$.

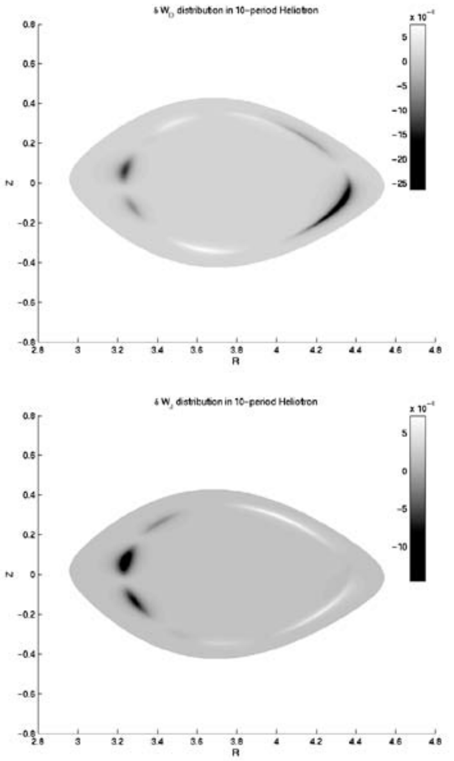

Fig. 2c The structure of the integrands of the functionals δW_D (top) and δW_J (bottom) for a 10-period currentless Heliotron on a toroidal cross section at midperiod ($\phi = \pi/10$). The scale for δW_D is $-2.6 \times 10^{-3} < \delta W_D < 7 \times 10^{-4}$ and the scale for δW_J is $-1.4 \times 10^{-3} < \delta W_J < 7 \times 10^{-4}$.

distributions of integrands of the functionals δW_D and δW_J in Figs. 2a–c on cross sections at the beginning, at one quarter and at midperiod. The most negative regions of δW_D concentrate at the tips of the elliptic cross sections corresponding to the locations where the magnetic field line curvature is most destabilising. This characterises the mode structure as ballooning. The most negative regions of δW_J concentrate at the inner edge of the torus and are a factor 2 smaller that δW_D. Though the Pfirsch-Schlüter current is formally proportional to p', the δW_J structure it drives does not display ballooning features. The observations made suggest where to physically position fluctuation detectors to identify the type of mode. In practice, heliotron systems like LHD [1] display finite currents due to neutral beam and

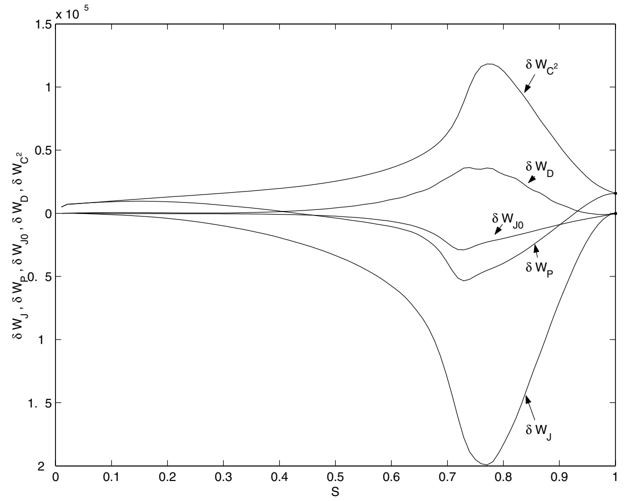

Fig. 3 The profile of the different components that contribute to the energy principle δW_P (the curves shown from top to bottom are δW_{C^2}, δW_D, δW_{J0} and δW_J, respectively) in a 2-period QAS reactor with finite bootstrap-like current.

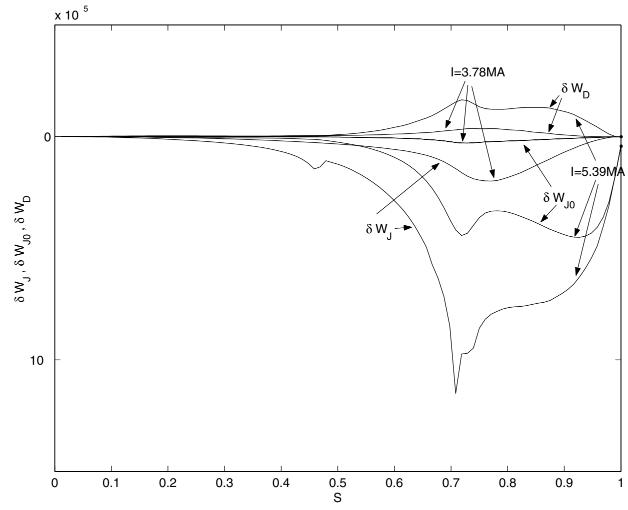

Fig. 4 The profiles of δW_D, δW_J and δW_{J0} in a 2-period QAS stellarator reactor with toroidal currents of 3.78 MA and 5.39 MA. The curves shown from top to bottom correspond to 1) (δW_D, 5.39 MA), 2) (δW_D, 3.78 MA), 3) (δW_{J0}, 3.78 MA), 4) (δW_J, 3.78 MA), 5) (δW_{J0}, 5.39 MA) and 6) (δW_J, 5.39 MA), respectively.

bootstrap effects. The impact of these currents will be addressed in future work.

4. Application to 2-period QAS with finitetoroidal current

We investigate a sequence of equilibria at $\beta \simeq 4.25\%$ computed with VMEC [7] with a fixed hollow bootstrap-like toroidal current profile that model a 2-period QAS stellarator reactor in which the magnitude of the current is varied arbitrarily. The formulation is valid also for peaked currents from neutral beam injection or ECCD in as much as the current profile and magnitude are prescribed as input to the VMEC code which computes selfconsistent equilibria. This procedure, in turn, affects the δW_J and δW_{J0} distributions when the stability is investigated using TERPSICHORE. However, we have not examined peaked current profiles in this paper. The bootstrap current causes the rotational transform profile to cross the critical $\iota = 1/2$ resonant surface whent the toroidal current approaches 3.8 MA and an external $m/n = 2/1$ kink becomes destabilised. The profiles of δW_P, δW_{C^2}, δW_D, δW_J and δW_{J0} are shown in Fig. 3 for a case with 3.78 MA toroidal current. The configuration is weakly unstable and driven primarily by the Pfirsch-Schlüter current because δW_J is dominantly negative and an order of magnitude larger than δW_{J0}. Surprisingly, on average the ballooning-interchange drive δW_D is positive, thus stabilising. Locally though, it is negative in regions of destabilising magnetic field line curvature. In Fig. 4, we display the profiles of δW_D, δW_J and δW_{J0} for the weakly unstable 3.78 MA current case and for a more strongly unstable 5.39 MA current case. It is seen that for higher currents that the contribution of the BC to the kink driving mechanism becomes more important and almost comparable in magnitude to that of the Pfirsch-Schlüter current.

5. Summary and conclusions

A diagnostic routine has been developed to analyse the stabilising and destabilising contributions to the ideal MHD Enery Principle using the eigenfunctions computed with the 3D TERPSICHORE code. The driving term can be separated into contributions from the parallel current density, which is responsible for kink modes, and the pressure gradient, which is associated with ballooning and interchange modes. The parallel current density contribution can be roughly separated into a Pfirsch-Schlüter term (which is proportional to the pressure gradient but does not generate a ballooning structure) and a flux surface average term associated with finite bootstrap, ohmic or ECCD currents. Test applications have been performed on a 10-period current-free Heliotron and on a 2-period QAS stellarator reactor with a fixed model bootstrap current profile and current magnitude that is adjusted arbitrarily. In the currentless Heliotron, the ballooning-interchange driving mechanism dominates that of the Pfirsch-Schlüter current. Furthermore, the ballooning-interchange destabilising energy concentrates in the region of weak magnetic field line curvature at the tips of the elliptic flux surfaces. The energy in the sub dominant Pfirsch-Schlüter current contribution localises at the inside edge of the torus. In the finite current QAS system investigated, the ballooning-interchange contribution is globally stabilising. The Pfirsch-Schlüter current contribution constitutes the main destabilising mechanism near marginal stability. For higher toroidal currents, the bootstrap current contribution to destabilise the kink mode becomes more important and can be quantified through the evaluation of the functional δW_{J0}. The different locations within the plasma where the unstable contribution of the kink driving term δW_J and the ballooning-interchange driving term δW_D concentrate can provide a very useful indicator of the type of unstable mode that can be detected from an experimental viewpoint.

Acknowledgements

The authors are thankful to Dr. S.P. Hirshman for the use of VMEC. This work was supported by the Fonds National Suisse pour la Recherche Scientifique and by Euratom. The computational results were performed on the NEC-SX5 platform at the Centro Svizzero di Calcolo Scientifico in Manno, Switzerland.

References

[1] A. Iiyoshi, A. Fujiwara, O. Motojima, N. Ohyabu and K. Yamazaki, Fusion Technol. **17**, 169 (1990).

[2] S. Okamura *et al.*, Nucl. Fusion **41**, 1865 (2001).

[3] A.H. Boozer, Phys. Fluids, **26** 496 (1983).

[4] W.A. Cooper, Plasma Phys. Control. Fusion **34** 1011 (1992).

[5] D.V. Anderson, W.A. Cooper, R. Gruber, S. Merazzi and U. Schwenn, Scientific Computing on Supercomputers II, Plenum Press, New York and London 159 (1990).

[6] Y. Nakamura, T. Matsumoto, M. Wakatani *et al.*, J. Comput. Phys. **128** 43 (1996).

[7] S.P. Hirshman and O. Betancourt, J. Comput. Phys. **96** 99 (1991).